Indian Journal of Chemistry
Vol. 59A, October 2020, pp. 1513-1528

Synthesis of metal oxide nanoparticles - A general overview

Debabrata Pal*
Department of Chemistry, Sreegopal Banerjee College, Bagati, Magra, Hooghly, West Bengal, India
Email: debu_magra@yahoo.co.in

Received 09 April 2019; revised and accepted 10 July 2020

Metal oxide nanoparticles (MONPs) are the most important class of nanoparticles regarding the volume of production and application potential in diversified fields. The research domain of MONPs is vastly expanding and rationally million of bytes are utilized to cover the literature each day around the globe. They can be synthesized in a variety of processes and the MONPs produced through different processes differ greatly regarding morphology, texture and functionality. Therefore fine tuning of process control in synthetic methodology is under extensive research along with relevant structures and properties so as to fit the need. Improvisations in synthetic procedures are always attempted and newer dimensions of applicability are being explored. The MONPs find extensive use in the field of optoelectronics, gas sensing, surface coating, biomedicine, fuel cells, catalysis and in so many fields. This review attempts solely to cover a general outline of the synthetic methods of production of MONPs and metal oxide nanostructures.

Keywords: Bottom up approach, Green synthesis, MONPs, Top down approach

Nanotechnology (NT) is undoubtedly the most developing domain of science for the present scenario. This field is utterly fascinating for researchers since the early 90s of the last century. NT has become the prime multidisciplinary branch of modern technology and surely it will encompass greater area in future. NT is considered as the "key technology of the 21st century". The prefix 'nano' is derived from the Greek word (Latin nanus), meaning "dwarf". A nanometer (nm) is an international system of units (Système international d'unités, SI), the unit that represents 10^{-9} meter in length. In principle, NT can be conceived as the subject dealing with the understanding and control of matter at dimensions between approximately 1 and 100 nm whereas nanomaterials (NMs) are commonly defined as any material having the confinement in the range of 1 to 100 nm in at least one of the three dimensions. Presently an internationally accepted single definition for NMs does not exist. As per the United States Environmental Protection Agency (US EPA), "NMs are a diverse class of substances that have structural components smaller than 100 nm in at least one dimension"[1]. According to The International Organization for Standardization (ISO TS 80004-1) the term 'nanomaterial' is proposed to be defined as "Material with any external dimension in the nanoscale or having internal structure or surface structure in the nanoscale"[2]. In the same line the Europian Union Commission, follows the definition as "Nanomaterial means a natural, incidental or manufactured material containing particles, in an unbound state or as an aggregate or as an agglomerate and where, for 50 % or more of the particles in the number size distribution, one or more external dimensions is in the size range 1 nm–100 nm"[3]. In this context, nanoparticles (NPs) are technically viewed as the materials having all three dimensions in the nano range and presumably NPs are the major class of NMs that attracted the scientific community from the advent of nanotechnology research.

Metal oxides are undeniably the most versatile class of chemical compounds with diversified structures and allied properties. The bulk properties of the metal oxides were studied with great deal. The crystal structure, thermodynamic stability, morphologies, associated electronic structure, electrical conductivity and other domains were well explored in order to tune the properties to fit the application. However, the advent of NT research extended the field of metal oxides to a more elaborated domain with incorporation of the term metal oxide nanoparticles (MONPs). The dimensional pre-requisite triggers new and robust research in terms of synthesis and stability of MONPs. The MONPs have emerged out to be of appealing properties different from that of the bulk

phase with great tunability and thus find extensive application in industry. In scaling down to nano dimension from bulk phase, a number of unique properties are developed in MONPs. These properties can solely be attributed to the size factor and the high density of sites at the corners or edge surfaces compared to bulk structure. The nano-dimensionality actually dictates three prime groups of properties in any material[4]. The first one is related to structure parameters, namely, the lattice symmetry, packing and the cell arrangement[5]. Bulk-phase oxides are thermodynamically very stable systems with robust array of atoms in a well-defined crystallographic framework. In descending down to nano range, the surface/volume ratio increases, resulting in huge modification of surface free energy along with distortion and strain arising out of the small size. These factors mutually determine the thermodynamic stability of the concerned nanostructure[6]. In the extreme case, the resulting alterations of the cell parameters and structural changes can be so huge, that a stable bulk phase structure may not be stable in the nano-range[7]. The strain arising out of greater atom density at the surfaces and corners due to size reduction is termed as internal strain[8]. Apart from this 'internal strain', an 'external strain' also develops depending on the method of synthesis. Calcinations and annealing may sometimes relieve them well[9]. The second group of properties, those changes remarkably upon scaling down is the electronic properties. The most important effect that the nano-dimension produces is the quantum confinement effect, which stems out of discrete, atom-like electronic states. These states can be conceived of as the superposition of bulk-like states with an associated increment of oscillator strength[10], leading to energy shift of excitation levels and optical band gap[11]. However, the long-range effect of the Madelung field which dictates the electronic properties of a bulk oxide surface, is practically nil or very small in nanoscopic oxdes[12]. A redistribution of charge evidently occurs in transition from long array periodic structure of bulk phase to small aggregates or clusters in nano phase, the effect being significant for covalent oxides and really small for ionic oxides[13]. The degree of iconicity in metal-oxygen bond is proposed to be controlled by the size of the matrix and increases with decrease in the size of the matrix. The third group of properties is attributable to size factor. Many oxides have broad band gaps and comparatively low reactivity in their bulk state[14]. A reduction in the average size of an oxide particle results in alteration of the magnitude of the band gap[15], with prominent influence on the conductivity and chemical reactivity[16]. Moreover, the size reduction results under-coordinated atoms (like corners or edges) or O vacancies in an oxide NP to suffice the specific geometrical arrangements. This alters the scenario of the occupied electronic states located above the valence band of the corresponding bulk material and the chemical reactivity is vastly enhanced[17,18]. Thus MONPs have evolved out as potentially multifunctional compounds and their functionality greatly depends on the particular states in which they are being formed[19-22]. There are always differences in size, shape, crystallinity, regularity as well as surface area, conductivity and several properties of a particular MONP depending upon the method of synthesis. Also the metal oxides in nano dimensions can be formed in polyphasic crystalline forms with oxides of different oxidation states of the metal. Sometimes mixed metal oxide NPs are synthesized as well as metal-metal oxide NPs where the metal oxide may be same or different to the parent metal[23,24]. The compositions can be stoichiometric as well as non-stoichiometric. They are better referred as metal oxide nanocomposites or metal oxide nano clusters[25]. The MONPs possess enormous technological applications as sorbents, sensors, ceramic materials, photo-devices and catalysts and so more.

Newer findings regarding the effectiveness of MONPs in diverse domains are being reported comprehensively. MONPs are being quite extensively incorporated in different nano frameworks in conjunction with different materials like Graphene[26,27], polymers[28,29], DNA[30,31], macrocyclic ligands[32] etc. They are also judiciously tailored in Metal Organic Framework (MOF) in order to evolve out novel properties[33]. MONPs are extensively utilized as Electron Transport Layer (ETL) for highly efficient Dye-Sensitized Solar Cells (DSSCs)[34]. They are also increasingly used to develop semiconductors[35]. The incorporation of MONPs with other functional materials proved to be innovative in the field of biomedical research, drug delivery, imaging and other fields. Lanthanide-Doped Hafnia NPs are reported for multimodal Theranostics and used for tailoring the physicochemical properties by interactions with biological entities[36]. Zhang et al. have reported the use of metal oxide nanoparticle band gap to develop a predictive paradigm for oxidative stress and acute pulmonary inflammation[37]. Gao et al. very recently showed the performance enhancement of Enzyme-Linked Immunosorbent Assay (ELISA) through use

of metal and MONPs[38]. A recent report also highlights the success of pharmacologic vitamin C-based cell therapy via iron oxide NP-induced intracellular Fenton reaction[39]. Archana et al. has efficiently employed hierarchical CuO/NiO-Carbon nanocomposite derived MOF on Cello Tape for the flexible and high performance nonenzymatic electrochemical glucose sensors[40]. The MONPs have also been utilized very effectively in different fields to attain better output. Adithya et al. reported the use of Lanthanum-iron binary oxide nanoparticles as cost-effective fluoride adsorbent and oxygen gas sensor[41]. Gnanasekaran et al. employed CeO_2, CuO, NiO, Mn_3O_4, SnO_2 and ZnO NPs as photo catalysts for degradation of textile dyes[42]. Gonçalves et al. also reported the photochemical H_2 production of Ta_2O_5 nanotubes decorated with NiO NPs by modified sputtering deposition[43]. The astonishing and diversified application potential of MONPs has prompted the research community to investigate keenly on newer synthetic routes and improvisations of the existing routes in order to achieve newer properties in a cost effective way. Greater emphasis in synthetic procedures is also employed to develop nano moieties where MONPs are incorporated within different functional materials. Another most important aspect of the synthetic procedures remains to produce MONPs in biocompatible form; therefore modifications in the synthetic protocols are always implemented to attain greater biocompatibility of MONPs.

Synthesis of MONPs

The synthetic regime of the whole domain of metal oxide nanocomposites can be primarily classified in two distinct divisions; the Top down approach and the Bottom up approach. Fig. 1 depicts the synthetic procedures of MONPs and the divisions there-in at a glance.

Top down approach

The top down approach generally covers the synthetic routes where the NMs are being formed from the bulk phase solid state precursors. It is the process of scaling down the bulk material to nano dimensions. There are a variety of processes through which the task can be performed. The top down approach is really very important for preparing the MONPs where very prolific and regularized shape of the NMs is required. In the top down approach, the starting material is essentially solid and there occurs slicing or successive cutting to get nano sized particles. There are mainly two techniques, mechanical techniques and lithographic techniques. Mechanical techniques comprises of cutting, etching, grinding, ball milling, whereas lithographic techniques are mainly electron beam lithography.

Mechanical techniques

Mechanical techniques refer to those processes where mechanical energy in the form of ball-milling is utilized to effect the desired change from macro to nano dimension. It can be classified into following sub-heads.

Mechanical milling

Mechanical milling is the method where a suitable powder charge (usually, a mixture of elements) is loaded in a high energy mill, in conjunction with a suitable milling medium in order to reduce the particle size as well as blending of particles in new phases (not always). The high energy rotating balls

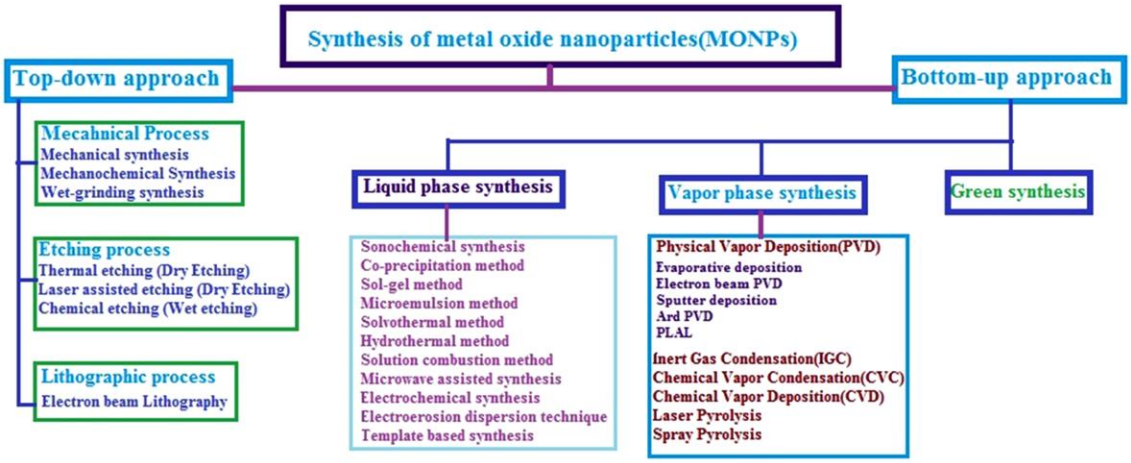

Fig. 1 — The classification of synthetic procedures of MONPs.

incur mechanical energy to the substituents promoting the collapse to shorter dimension. Depending on the energy input, the process can be hard as well as soft. The method was first developed by John Benjamin (1970) and co-workers at the International Nickel Company in the late 1960's in order to synthesize complex Oxide Dispersion-Strengthened (ODS) alloys and production of fine, uniform dispersions of oxide particles (Al_2O_3, Y_2O_3, ThO_2) were reported.[44] Lee et al. reported the size reduction from commercial 1 μm α-Fe_2O_3 powder (99.9%) to about 15 nm in 100 h ball milled powder along with α-γ-α-Fe_2O_3 transformations[45]. Indris et al., also reported the synthesis of nanocrystalline powder of the anatase and rutile modifications of TiO_2 in the average grain size of 20 nm through high energy ball milling of the coarse grained sample for upto 4 h[46].

Mechanochemical method

Mechanochemical method is a method where a chemical process is performed through activation by mechanical ball miling[47]. This method does not require any thermal input. The displacement reaction occurs in the solid phase. The prime advantage of mechanochemical synthesis lies in the fact that agglomeration does not take place as compared to other methods. Very pure NPs are produced by this method with easier control of particle size distribution by optimization of parameters like ball to powder weight ratio, stoichiometric ratio of starting materials, milling time and intervals together with other factors. The particles formed during mechanochemical synthesis are disperse and nanocrystalline because of pulverization of the reagents and chemical interaction between the components. After the completion of milling, the NPs are obtained as dispersed within the soluble salt matrix being surrounded by by-products. Selective disposal of the matrix phase is carried out by washing the produced powder with suitable solvents. Solvents are dried off and characteristization is the next step. An outline of the process can be given where Fe_2O_3 NPs have been synthesized by mechanochemical solid-state reaction between sodium carbonate (Na_2CO_3) and iron chloride ($FeCl_3$, $6H_2O$)[48]. Various types of MONPs and metal-metal oxide nanocomposites have been synthesized by this method, e.g., CeO_2[49], ZnO[50], $CoFe_2O_4$[51] etc.

Wet grinding method

Wet grinding method is another good method, where the bulk phase metal oxide is grinded in presence of a surface modifier to get the MONP. Priyadarshana et al. have synthesized magnetite NPs from a high purity natural iron oxide ore found in Panvila, Sri Lanka through five-phase controlled grinding in presence of oleic acid as surface modifier following a novel top down approach. Oleic acid, a long chain carboxylic acid hinders the process of agglomeration and oleic acid coated magnetite NPs are obtained in the size distribution of 20–50 nm[52].

Etching method

Etching synthesis refers to the scenario where the surface of the precursor material or unprotected parts of the pre-treated micro-sized precursors (generally referred as wafer) are cut off either by physical methods or chemical methods to effect fabrication on the surface of the wafer. The pre-treatment requires the specific patterns to be deposited as masks on the wafer surface, which are done through lithography. Thereafter the physical methods or the etchant are used to cut off the unprotected regions of the wafer surface to develop the final fabricated NM. Etching can be categorized as dry etching using physical methods and wet etching using chemical etchant.

Dry etching

Thermal etching is categorically considered as a method of dry etching. Thermal etching is the case where some sort of surface modification of MONPs/nanocomposites via removal of oxygen from the surface sites is achieved through annealing. In case of metal oxides like ZnO, oxygen (O) vacancy is formed via O_2 evaporation from lattice that leaves behind negative charges. These O vacancy sites are very much favorable for H_2O adsorption and consequent metal ion detachment from the lattice resulting in enhanced macroscopic dissolution. In ZnO NPs, under annealing in an air/fluid heating system in the temperature range of 303 K to 363 K using ultrapure water, deeper and larger etching pits are formed with increasing temperature and can be correlated to increase in O vacancy sites, promoting greater dissolution[53].

Laser assisted etching

When laser is utilized for the etching purpose, the process is laser assisted etching. Here laser rays bring about inelastic collision with the lattice surface that results in fragmentation of the lattice to smaller domain as well as modification of the lattice. Co_3O_4 NPs were synthesized by means of laser fragmentation from raw Co_3O_4 powders at room

temperature[54]. The laser source, as reported, was a nanosecond pulsed Nd:YAG laser (Dawa-350 from Beamtech) with wavelength of 1064 nm, pulse width 7 ns, and power density of 6×10^7 W cm^{-2}.

Wet etching

Chemical etching falls under the category of wet etching. This is indeed another method where highly regulated shape of the NMs can be obtained. Chemical etching is the process where the etchant, mainly strong acid or mordant (a corrosive liquid) is employed for the purpose. The etchant dissolves or etches out portions of the unprotected surface of the as prepared micro-sized precursors (wafer) to transform the precursor into nano range with desired fabrication on the surface. Wang et al. reported the in situ synthesis of the ZnO nanotips array with number density of about 4×10^8 cm^{-2} from $ZnCl_2$ and ammonia by seed-layer assisted growth technique.[55] Kwangjin et al. also reported the synthesis of various hollow oxide NPs from as-prepared MnO and iron oxide nanocrystals by heating the metal oxide nanocrystals dispersed in technical grade trioctylphosphine oxide (TOPO) at 300 °C for hours. The impurities in technical grade TOPO, especially alkylphosphonic acid, was found to be responsible for the etching of metal oxide nanocrystals to the hollow structures[56]. Li et al. demonstrated a facile top-down etching method to fabricate the uniform single crystal hematite concave nanocrystals[57]. The selective etching along [006] zone axis of the icositetrahedron was made possible by employing phosphate ions as an effective etchant. α-Fe_2O_3 hexagonal hollow rings were also synthesized by this top down etching approach.

Lithographic techniques

Lithography is the method of transferring a specific pattern from one to another media. Electron beam lithography emerged in the 1960's. It comprises of the electron beam irradiation on a surface that is sensitive to electrons by means of scanning with focused electron beam which results in differential absorption of energy from the electron beam together with physical and chemical changes. The process ultimately creates a latent image of the desired pattern on the surface, called resist, which on subsequent physical or chemical treatment produces the ultimate fabrication on the surface. The fabrication of metal oxide nanostructures with precisely controlled geometries and spacing is very important in the improvement of functionality. A study is exemplified where sputtered TiO_2 thin films of 130 nm thickness deposited on Silicon wafers covered with thermally oxidized SiO_2, were patterned using direct write e-beam lithography combined with dry etching in an inductively coupled plasma (ICP) system[58]. The designed motives with dots diameter from 45 to 200 nm and spacing from 200 to 2000 nm were defined into HSQ negative resists at various thickness.

Bottom up approach

The bottom up approach encompasses the synthetic routes that start from the fundamental building blocks, mainly atoms and molecules[59]. The precursors are initially brought in the molecular range from where the process of self-assembly hierarchically develops the NM. The bottom up approach can be subdivided into three categories; liquid phase synthesis, vapor phase synthesis and green synthesis. Although green synthesis is exclusively liquid phase synthesis, yet it is categorized in a different class. Whether it is a liquid phase synthesis or vapor phase synthesis, two routes are followed; the chemical route and the physical route. Liquid phase synthesis always involves chemical route, whereas the vapor phase synthesis involves the physical route except chemical vapor deposition and pyrolysis.

Liquid phase synthesis

Liquid phase synthesis involves the process where the precursors are in liquid matrix[60]. Solutions of metal salts and organometallic compounds with suitable solvents are the starting material, which then undergo the chemical transformation by providing activation energy by different means. According to the type and source of energy supply, different terminologies are attributed to different bottom up synthetic routes. The chemical transformation leads to formation of metal oxide products. The nucleation and growth are the fundamental controlling aspects that are adjusted so as to minimize agglomeration by providing the supply of surfactants and/or modifier and/or capping agents in the reaction medium if necessary. The next part is the work-up followed by characterization of the NM. The conventional liquid phase synthetic routes are described below. However modern day synthesis in most of the times involves more than a single route coupled together for better synthetic results.

Sonochemical method

In sonochemical method, the metal salt is subjected to very strong ultrasound vibration that causes the

breaking of the chemical bond. The acoustic cavitation resulting from alternate compression and relaxation together with the immense change of pressure and temperature in very short zones within ultra-short time-period in the solvent matrix leads to reaction. It is subsequently followed by nucleation but growth is hindered and the particles are produced in nano dimension[61]. In general, high temperature and pressure are not required and synthesis time is short. This method also provides a way of synthesizing monodisperse NPs of uniform size and high surface area. Surfactant addition is not necessary and the NPs are obtained in crystalline phase. A variety of MONPs have been synthesized by sonochemical method. Examples may be cited of preparation of ZnO NPs by reaction of zinc acetate with sodium hydroxide. The mixture is first sonicated for 35 minutes by 60 W ultrasound power and milky white precipitate of zinc hydroxide is produced. The precipitate upon subsequent washing and anneling at 400 °C, produces white powder of ZnO NPs in the average size of 57.5 nm[62]. Other examples include formation of NiO[63], TiO_2[64], CeO_2[65] etc.

Co-precipitation method

Co-precipitation method is one of the most widely used methods for obtaining MONPs. This involves the reaction between a metal salt precursor (mainly nitrate or chloride) with base in aquous medium in presence of surfactant and /or capping agent in mild thermal conditions. Metal oxo-hydroxide is obtained which upon oven-drying, MONPs are produced. This is the most efficient way for preparation of magnetite NPs. The pH and ionic strength of the medium are important for precipitation. The nucleation and growth are the two important factors that are needed to modulate in order to hinder agglomeration of the NPs. The particle size can be adjusted within the range of 20 nm. Massart et al. first synthesized superparamagnetic iron oxide NPs of spherical shape with diameter of 8 nm by alkaline precipitation of $FeCl_3$ and $FeCl_2$[66]. Various MONPs have been synthesized by this method, some representative examples may be given regarding synthesis of ZnO[67], MnO_2[68], SnO_2[69] etc. A synthesis quite similar in principle to the method of co-precipitation has been devised which worked in absence of solvent. A hydrated metal salt (typically a nitrate or chloride salt) is mixed with bicarbonate (generally NH_4HCO_3) thoroughly for 10–30 minutes to transform into the precursor from which upon calcination at quite low temperatures (220–550 °C) for 1–3 h, the NPs are produced. MONPs of most of the transition metal and semi-metals in the periodic table (groups 3–4 and 6–15) as well as some of the lanthanide group metals can be synthesized by this solvent-less method[70].

Sol-gel method

Sol-gel method is a widely recognized method for the synthesis of MONPs[71]. The process involves the hydrolysis of metal reactive precursors, mostly alcoholic solution of alkoxides that break down to the corresponding hydroxide upon hydrolysis. Condensation of the hydroxide molecules by removing water molecules forms a network of metal hydroxide. Gelation is achieved in the process of polymerization of the hydroxide species through condensation of the hydroxy network and a thick porous gel is resulted. Elimination of solvents and proper drying of the gel are very important steps that produces an ultra-fine powder of the metal hydroxide, which upon heat treatment in the final step leads to the corresponding ultra- fine powder of the metal oxide. This method has been utilized for preparation of a number of MONPs and nanocomposites like TiO_2[72], ZrO_2[73], MgO[74], $InNbO_4$[75] etc.

Microemulsion method

This method deals with two immiscible phases (oil and water), separated by a monolayer of surfactant molecules and thus forming two binary systems—water/surfactant and oil/surfactant—in a way that the hydrophobic tail groups of the surfactant molecules are dissolved in the oil phase whereas the hydrophilic head groups are in the aqueous phase[76]. The typical examples for emulsifier/surfactant are sodium dodecyl sulfate (SDS) and aerosol bis(2-ethylhexyl) sulfosuccinate (AOT). This method involves mixing of appropriate amounts of the surfactant, oil, water and the metallic precursor (e.g. organometallic precursor solution in the oily phase) followed by stirring at room temperature to develop a homogenized phase. When the concentration of the emulsifier in water (or oil) solutions are small, the emulsifier is soluble and exists as a monomer, but when the concentration exceeds the critical micellar concentration (CMC), the spontaneous aggregation of the emulsifier molecules results in formation of micelles and these micro-water droplets serve the role of nanoreactors for the formation of NPs[77]. Addition of reducing/ oxidizing/precipitating agents in the homogenized phase with vigorous stirring do the task of exceeding the CMC and results in precipitation of the NPs

within the micelle core, which follows centrifugation, wash cycles and drying/ calcinations to the ultimate production of the NPs. The formed NPs are generally mono-disperse. Shape and size can be modulated in these methods by regulating the various self-assembled structures produced in the binary systems. Varieties of MONPs have been prepared by this method like ZnO[78], CeO_2[79], CuO[80] etc.

Solvothermal method

Solvothermal method is the method where the reaction mixture in the solvent is treated in an autoclave at an elevated temperature less than the boiling point of the solvent at higher pressure[81]. The conditions in the closed container greatly change the solvent properties approaching the critical state and thus product formation becomes more facile. In case of MONPs, metal precursors with appropriate reagents are heated in autoclave, sometimes in presence of polyols and surfactants that serve the role of capping agent. Solvothermal synthesis of single-crystalline ZnO nanostructures have been reported, where using methanol as solvent, ZnO nanorods with length and width in the range of 100–150 nm and 20–25 nm respectively, are produced from zinc nitrate and zinc acetate, although ZnO NPs of diameter 20–25 nm are produced from zinc chloride under similar condition. Changing the solvent to ethanol, exclusively produces NPs from all precursors[82]. Iron oxide NPs have also been synthesized by alkaline solvothermal method employing anhydrous ferric chloride, sodium hydroxide, polyethylene glycol and cetyl trimethyl ammonium bromide, the product being a mixture of different phases of iron oxides namely γ-Fe_2O_3(maghemite, tetragonal), Fe_2O_3 (maghemite, cubic), Fe_3O_4(magnetite, cubic) and ε- Fe_2O_3 in size range of 19.8 nm to 48 nm[83]. Other examples include synthesis of TiO_2[84], CeO_2[85] etc.

Hydrothermal method

Hydrothermal method is the name given to the solvothermal process when water is employed as the solvent. In most cases the hydrothermal method consists of decomposing organometallic precursors. The major advantage with organometallic compounds being that the precursors can be treated at relatively low temperatures to form the final product. The control of the decomposition temperature and pressure allows the tuning of the properties of the NPs regarding size and morphology. Hydrothermal processes can be modulated in two types of systems; the batch hydrothermal and continuous hydrothermal process. In the first case, the process can be continued with the desired ratio phases while for the latter a higher rate of reaction can be achieved at a shorter time period. As for example TiO_2 NPs have been synthesized in the hydrothermal method by the hydrolysis of titanium tetraisopropoxide (TTIP) using HNO_3 as a peptizing agent[86]. Other examples can be cited regarding formation of ZnO[87], MgO[88], Co_3O_4-ZnO NP-composite[89] etc.

Solution combustion method

Solution combustion synthesis (SCS), being a time-saving as well as energy-saving process as compared to other routes, is employed for the formation of complex oxides with scale-up applications. Solution combustion method comprises of an exothermic reaction between metal precursors and organic fuels. The combustion reaction initiates by decomposition of metal precursors and fuels to the intermediate products that are solid-reacted by the thermal energy evolved during the exothermic reaction to generate the final product. The molecular mixing of cations together with fuel chelation dictates towards the formation of the product following calcination at lower temperatures[90]. In a recent work, iron oxide NPs have been synthesized by one pot solution combustion method using ferric nitrate (as metal precursor and oxidizer) and glycine (as fuel) where control over the morphology and composition had been tuned by only adjusting the molar ratio of fuel (glycine) to oxidizer (ferric nitrate)[91]. Other examples include synthesis of ZnO[92], TiO_2[93], MgO[94] etc.

Microwave assisted synthesis

Microwave assisted synthesis is referred to any of the earlier discussed solution based synthetic procedures for which the energy input is provided by microwave heating. It is also termed as dielectric heating, since only dielectric substances can absorb and interact with microwave radiation and is a non-quantum mechanical phenomenon. It is a process where direct heating rather than conductive heating can be achieved instantaneously. Microwave irradiation can produce high temperature and rapid cooling on just a switch and this short durational direct high energy input triggers the product formation. It has been proved to be a very purposeful way to synthesize NPs and to modulate their shape, size and morphology accordingly. Singh et al. had reported the synthesis of SnO_2 NPs by microwave heating. A

precursor solution was made by dropwise addition of 0.05 M citric acid to a 0.03 M solution of $SnCl_2.2H_2O$ and the mixture was heated at 80°C in oven to reduce the volume to one-fourth of the initial. Microwave treatment at 700 watt for 10 min on the precursor solution mixture produced precipitate, followed by washing, drying and subsequent annealing at 500 °C produced the NPs[95]. The microwave heating are now employed in conjunction with other processes for providing in situ 3D heating, which proved to be very useful for manufacture and fabrication of well-dispersed metal oxide NPs on a 3D carbonized wood[96]. Other examples of MONPs synthesized via microwave heating include ITO[97], ZnO[98], Co_3O_4[99] etc.

Electrochemical synthesis

Electrochemical synthesis is a rather old technique for formation of MONPs, especially to produce coatings of MONPs over substrate surface. This electrochemical synthesis of MONPs is very promising towards fabrication of the surface to sophistication and desired accuracy. The process is very facile and fast, occur at room temperature, less time consuming and above all impurities can be restricted. The shape and morphology of the nanostructures can be modulated by controlling different parameters. The general techniques are (a) pulse current deposition to control the growth of deposits, (b) use of additives and surfactants to modify the grain size of deposits and (c) NPs insertion into deposits to form nanocomposites. These electrodeposition techniques play a major role towards fabrication of electrodes for use in different types of sensors. Park et al. reported the electrodeposition of randomly oriented polycrystalline maghemite (γ-Fe_2O_3) NPs with the control over the morphology and production rate of NPs by altering the current density and the electrolyte compositions[100]. Yang et al. also reported the synthesis of a composite Cu_2O/TiO_2 electrode by electrodeposition of helical TiO_2 nanotubes array (diameter ≈ 105 nm) by anodic oxidation followed by deposition of layer of Cu and Cu_2O mixture with an approximate thickness of 100 nm with potential electrocatalytic activity toward glucose oxidation[101]. Among other metal oxides synthesized in nano dimension by electrodeposition are ZnO[102,103], tin oxide[104] etc.

Electroerosion dispersion

Electroerosion dispersion is the technique in which granulated metal is transformed into powder by electrical discharge. Typically a few hundred volts are discharged in the time limit of a microsecond, resulting to attain the plasma temperature in the discharge filament around 10000 to 15000 K that suffice to melt any metal[105]. Halbedel et al. has recently reported the synthesis of iron oxide powders in the form Fe_2O_3 in the size range of 20–50 nm by electroerosion dispersion of carbon steel in tap water[106].

Template based synthesis

Template based synthesis routes emerged out quite recently under the thrust to cater multidimensional applicability regarding improvised mechanical, optical, magnetic, and electronic properties that can be boosted through structure modifications of NMs. The templates serve as the guiding pattern of the way the NPs will be formed and in this strategy the NMs are synthesized within the pores or channels of the nanoporous template. Depending on the properties of the template, NMs in different morphologies such as rods, fibrils and tubules can be prepared. Track-etch membranes, porous alumina and other nanoporous structures serve the role as templates and different strategies like electrochemical and electroless depositions, chemical polymerization, sol-gel deposition and chemical vapour deposition have been utilized for template directed synthesis of MONPs[107]. Qi et al. recently reported the synthesis of hierarchically nanotubular MoO_3/SnO_2 composite based on the layer-by-layer self−assembly process of molybdenum trioxide nanocrystallites immobilized as a thin layer on the tin oxide nanotube surface employing natural cellulose substance(commercial filter paper) as structural scaffold followed by a calcination treatment[108]. MONPs like MnO_2 and Gd_2O_3 have also been synthesized in a facile environment-benign strategy by employing keratin, a family of cysteine-rich structural fibrous protein, as a platform template for the first time[109]. Blue-emitting ZnO NPs with a particle size of 12–36 nm have been synthesized employing cellulose bio template derived from *Azadirachta indica* (neem) leaf extract prepared in different solvents[110]. Anatase TiO_2 NPs have also been synthesized by using poly-acrylic acid hydrogel as template at room temperature in a cost-effective procedure[111]. α-Fe_2O_3 NPs of less than 5 nm size have also been produced by a template-assisted combustion method employing iron and ammonium nitrate as oxidizers, glycine as fuel and mesoporous silica (SBA-15) as template[112].

Vapor phase synthesis

Vapor phase synthesis comprises a very important strategy to produce MONPs. As the term suggests, here the actual process of NP formation occurs in the vapor phase. The precursors should be in gaseous phase or should be converted to gaseous phase if solid or liquid precursors are used as the case may be. The main components of vapor phase synthesis are the precursor, vaporizer and the support matrix. The precursor is the metal precursor from which nanodimensional metal oxide is sought to be produced. The vaporizer is the physical part of the process, it leads to generation of the vapor of the substrate. The vaporization may be induced by thermal process, ion beam, laser, plasma arching etc. Presence of oxygen in the processing device is a must for MONP formation. There may be some chemical reactions among the gaseous components or the physical processes alone can produce the metal oxide in the vapor phase. Supersaturation of the vapor is a key to condensation in the vapor phase followed by nucleation and growth to produce the NPs. The physical conditions are so adjusted that the condensation occurs guidedly on support matrix or target. Matrix supported thin layers, nano films, nano clusters are obtained in this process. The vapor phase synthetic routes are conventionally subdivided in following heads.

Physical vapor deposition

Physical vapor deposition (PVD) is an atomistic deposition process and commonly attributes to all those processes that employ a physical driving mechanism of the vapor phase of the material. The material is vaporized from a solid or liquid source and then transported in vapor form through low pressure gaseous (or plasma) environment to the substrate in the process chamber. Here condensation occurs in the gas phase due to multibody collision followed by nucleation and growth resulting in ultimate solid phase deposition on the substrate. PVD is considered as a major tool towards fabrication of nanostructures in surface coating. The first component of PVD process is an energy source that vaporizes the material from solid state and accordingly the processes are categorized as thermal evaporation, electron beam evaporation, sputtering, ion-plating, ion-assisted sputtering and laser ablation etc., depending on the type of energy source and mechanism being used for the process of vaporization. The vaporization process and transport of the vapor are carried out in very low pressure to ultra-high vacuum that eliminate least chance of impurity contamination as well as provide a long mean free path of the vapor particles to get deposited preferentially at the target substrate which is placed away from the source. The Physical vapor deposition technique has emerged out to be a very advantageous process for high deposition rate of surface coating and to get thin films with high purity and adhesivity with ease of instrumental automation.

Evaporative deposition

Evaporative deposition or thermal evaporation is actually the PVD process where thermal means is employed for vaporization. In this process micro-sized or powder phase of source material is vaporized at elevated temperature generally below the melting point and the resultant vapor phase condenses in presence of oxygen depending upon temperature, pressure and environment of the medium. Evaporation time and flow rate of the gas phase are crucial parameters that dictates the product deposition. The thermal evaporation process is very susceptible to the concentration of oxygen in the growth environment. The differential concentration of oxygen controls the volatility of the source material as well as the stoichiometry of the vapor phase. Fouad et al. reported the deposition of ZnO thin films of about 10-80 nm size on silicon substrate from metallic Zinc (≈ 5mm × 5mm, 99.5% purity) by thermal vapor deposition technique with total pressure of 5×10^{-3} torr and temperature ranging from 350 to 650 °C[113]. Zhang et al. also reported the synthesis ZnO nanorods using simple thermal evaporation at 650 – 850 °C for 60 to 120 min[114]. Hematite (α-Fe_2O_3) thin films were deposited by the reactive evaporation of iron in an oxygen atmosphere[115]. Thin films of CuO were deposited by thermal evaporation of cuprous oxide (Cu_2O) powder[116]. TiO_2 thin films were also synthesized by vacuum evaporation technique on glass substrates at room temperature[117].

Electron beam PVD (EBPVD)

In electron beam evaporation, the evaporative heating is achieved via an electron beam which is targeted on the anode made up of the material to be deposited, in high vacuum of the order of 10^{-6}–10^{-9} torr. It creates a high vapor pressure of the depositing material through snatching of the atoms from the solid surface by means of electron bombardment. The resulting vapor transports through the process chamber and deposits as the top-coating on substrate surface. The instrumentation comprises of the control of

electron beam energy, distance between target and substrate, substrate temperature and orientation and most importantly the order of vacuum. These factors play the key role towards the morphology of the produced NPs. Regarding synthesis of MONPs by EBPVD, the presence of oxygen is a prerequisite and generally O_2 gas at a pressure in the order of 10^{-5} torr is introduced in the deposition chamber, that suffice for the formation of metal oxide nanodeposits. Yang et al. reported the deposition of crystalline anatase TiO_2 film with 0.5×10^{-4} torr of O_2 pressure by electron-beam evaporation using rutile TiO_2 as a source material[118]. Tesfamichael et al. reported the preparation of pure tungsten oxide (WO_3) and iron-doped (10 at.%) tungsten oxide (WO_3:Fe) nanostructured thin films using a dual crucible electron beam evaporation (EBE) technique at room temperature under high vacuum onto glass as well as alumina substrates followed by annealing at 300 °C for 1 h[119]. Both α-Fe_2O_3 thin films and nanorod arrays have been deposited using electron beam evaporation through normal thin film deposition and oblique angle deposition[120].

Sputter deposition

Sputtering is the process that falls under physical vapor deposition category. Mechanistically sputtering involves the ejection of atoms or molecules of a material by bombardment with high-energy particles on the target material under very low pressure condition. In case of cathodic sputtering, the bombardment is furnished by positive ions derived from an electrical discharge in a gas. The atoms are ejected away from the target and transported through the process chamber to final deposition on the substrate surface. Sputtering includes diode sputtering, ion-beam sputtering, magnetron sputtering, cathodic sputtering, KF or DC sputtering, reactive sputtering - but all these follow the same physical phenomenon on principle[121]. In magnetron sputtering, which is employed in maximum, the magnetron uses the principle of applying a specially shaped magnetic field to a diode sputtering target. Metal oxide thin films in nano dimension can be prepared by various sputtering methods. ZnO/Ag_2O composite thin films with different Ag_2O contents have been successfully synthesized on non-woven fabric at room temperature by radio frequency (RF) sputtering with a single ceramic target formed by hot pressing ZnO/Ag_2O nanocomposite powder in Ar atmosphere at 180 °C for 30 min[122]. Shivya et al. reported the synthesis of magnetron sputtered CdO thinfilms for ammonia sensing[123]. Rydosz et al. also reported the preparation of CuO, TiO_2 and SnO_2 thinfilms by magnetron sputtering for sensing purpose[124].

Cathodic arc deposition or Arc PVD

Cathodic arc deposition or Arc PVD is also termed as cathodic plasma deposition. It is one among the oldest of coating technologies and improvisations in this field is astonishingly remarkable, such that it can be termed as the most emerging coating technology in the modern times, too. Cathodic arc plasma deposition categorically belongs to physical vapor deposition (PVD) techniques, although one point should be clear that it is a plasma deposition involving energetic condensation from plasma ions, rather than condensation of atoms from the vapor phase as in principle of PVD. The cathodic-arc deposition occurs between two metallic electrodes in vacuum (~10^{-3}–10^{-4} torr). A cathodic arc is a low-voltage, high-current plasma discharge. The arc current is concentrated at discrete sites at the cathode. These sites are termed as cathode spots and range ~1–10 μm in size. The current passing through a cathode spot amounts to 1–10 A. A typical arc discharge current of nearly 100 A produces a dense plasma of the cathode material. The ions within the plasma with substantial kinetic and potential energy get deposited in the form of thin film with unique properties. Diaz et al. reported the chromium and tantalum oxide nanocoatings prepared by filtered cathodic arc deposition for corrosion protection of carbon steel[125]. Among other metal oxide nanofilm coatings that have been developed by pulsed arc vacuum plasma deposition includes Titanium oxide[126,127], Cupric oxide[128] etc

Laser induced synthesis – PLAL (Pulsed Laser Ablation in Liquids)

Laser induced synthesis applies to all synthetic methodologies in the PVD category that employ laser in some way as the energy source to create the vapor phase of the material for the production of the NM. Different terminologies have been evolved out according to the mechanistic ins and outs of the processes, such as pulsed laser deposition (PLD) in gas chamber, laser vaporization controlled condensation (LVCC) etc. The efficacy of laser as an energy source depends on the wavelength, intensity, coherence and most importantly on the pulse width of the laser. A general name of pulsed laser ablation (PLA) for all laser induced PVD process is an accepted formalism. The PLA generally refers to ablation of the solid target by means of laser in the form of plasma plume, which is carried forward near

to the substrate followed by supersaturation leading to nucleation and growth of the NM on the substrate. The laser ablation of solid material can occur in gaseous as well as in liquid matrix. However, the liquid matrix offers a great many advantages to control the physical and chemical processes occurring at the liquid-solid interface and that is why pulsed laser ablation in liquid (PLAL) has evolved as the most convenient way of NP synthesis. The choice of the liquid has a great influence on the shape, size, morphology and properties of the formed NPs. The synthesis occurs at room temperature, high pressure is generally not required. It is an environment friendly process and synthesis time is short. However, the chance of large scale synthesis is very much limited. Huge number of MONPs and nanocomposites have been prepared by PLAL. Examples may be given to synthesis of ZnO[129], SnO_2[130], TiO_2[131], CdO[132] etc.

Inert gas condensation

The technique of inert-gas condensation (IGC) involves evaporation of the solid phase material by thermal means or sputtering or by means of laser ablation inside the process chamber maintained at very low pressure of the order of about 10^{-7} torr. The process chamber is subsequently back-filled with a low-pressure inert gas like helium at low temperature resulting in dissipation of the kinetic energy of the material atoms by collision with the inert gas atoms inside the chamber. This energy loss leads to condensation in the form of small particles. The condensed particles are collected on a cold finger, kept at liquid nitrogen and the deposit is scraped off into a collection unit. The crystal size of the powder is generally in the range of a few nanometers and the size distribution is typically narrow. The crystal size depends on the inert gas pressure and temperature, the relative rate of evaporation and the gas composition (% of inert gas). High pressure and high molecular weight of the used inert gas leads to increase in particle size. A wide range of MONPs and nanocomposites have been synthesized by condensation of nanosized amorphous particles and their successive compaction by applied high pressure. Ramasamy et al. reported the synthesis of Sn-doped In_2O_3 (ITO), ZnO, Al_2O_3, Ag_2O, CdO, CuO in the form of nano deposits by IGC technique[133]. Kusior et al. reported the deposition of Sn and Cu oxide nanoparticles on TiO_2 nanoflower 3D substrates by IGC technique[134]. A. I. Ayesh also reported the synthesis of CuO clusters by IGC technique in high vacuum[135].

Electromagnetic Levitation Gas Condensation (ELGC)

Electromagnetic levitation melting gas condensation (ELM-GC) or electromagnetic levitation gas condensation (ELGC) is an improvised modern version over conventional ICG. This process is devised in a way that no sample holder is required. Here the metallic sample is kept prepositioned in an electromagnetic field produced by induction coils of suitable geometry. The sample is melted and levitated stably. The vapors resulting from the evaporation of the molten levitated sample collide with the inert cooling gas blown directly on to the molten droplet surface and condensation occurs in the form of high purity fine powder of ultra small size. The size of the NPs depends on the droplet temperature and also quite strongly on the flow rate and heat capacity of the carrier gas. Various MONPs and nanocomposites have been synthesized by this method, examples may be cited regarding formation of ZnO[136,137], γ-Fe_2O_3 [138], $NiFe_2O_4$[139] etc.

Chemical vapor condensation (CVC)

In chemical vapor condensation, vapor phase components, produced mostly from solid phase precursors by resistive heating or by means of laser, plasma etc., are carried into a hot-wall reactor equipped process chamber, where nucleation of particles in vapor phase occurs that follow condensation in the form of ultra small particles. The conditions are so adjusted such that deposition in the form of thin film on the reactor wall can be minimized. The chemical reaction occurs between the gaseous precursors at high temperature in the gaseous phase and the resulting by-product gaseous substances are blown away after condensation. Metal salt or the metal itself can function as the role of precursor and presence of oxygen is a prerequisite for formation of oxides. Metal oxide nanobelts, nano fibres are the major types of thrust approach of CVC. This process is also referred as solid-gas-solid or gas-solid condensation. Hussain et al. reported the synthesis of hexagonal and tetragonal crystals of alkali metal tungsten bronzes M_xWO_3 (M=K, Rb, Cs), employing several transport agents like $HgCl_2$, $HgBr_2$, HgI_2, Cl_2, $PtCl_2$ in a temperature gradient. The hexagonal crystals were developed upto 6 nm whereas the tetragonal crystals upto 0.1 mm[140]. Wang et al. also reported the synthesis of ultrasmall single-crystalline ZnO nanobelts of ~ 200 nm in width by a facile

gas-solid condensation employing thin film of metallic tin as catalyst[141]. Fe/TiO_x and Fe-Co/TiO_x nanocomposites were also reported to be synthesized by gas phase condensation in ultra-high vacuum chamber from Fe (99.9%), Ti (99.9%) and Co (99.9%) powders, whilst He (99.9996% purity) and O_2 (99.9999% purity) being supplied into the pre-evacuated chamber (~2 × 10^{-7} torr) maintaining the total pressure at ~2 torr with the help of a rotary pump[142].

Chemical vapor deposition (CVD)

Chemical vapor deposition (CVD) is the process that is extensively used for thin film deposition of NMs over the surface of substrate or wafer. A CVD system is comprised of a precursor supply system equipped with a CVD reactor and exhaust machinery. In the case of CVD, liquid precursors are mostly used in order to achieve sufficient vapor pressure by heating at intermediate temperature, generally below 200°C. Multiple precursors can also be used following the course of the reaction. Liquid substances with low volatility or solid precursors can also be introduced in the form of liquid injection-CVD and aerosol assisted-CVD. The deposition reaction takes place within the reactor among the vapor phase precursors and the external energy is provided by thermal means or light or plasma. Deposition occurs homogeneously and in some cases heterogeneously which in turns governs the uniformity and adhesivity of the deposited film. The exhaust machinery is utilized to swipe off the gas phase reaction by-products. The morphology of deposited film is influenced by ambient pressure in the CVD chamber, the temperature of the vapor and the substrate, by the nature of substrate surface and also by the heat capacity and molecular weight of the carrier gas. Multi-component oxide nanosystems are synthesized in the most versatile fashion by CVD technique[143]. Barreca et al. reported the synthesis of ZnO-TiO_2 nanocomposites by CVD through an initial growth of ZnO nanoplatelets on Si(100) and Al_2O_3 substrates, followed by dispersion of TiO_2 nanoparticles over the initially grown ZnO nanoplatelets at a temperature of 350°C – 400°C from $Ti(O^iPr)_2(dpm)_2$ [O^iPr : iso-propoxy; dpm : 2,2,6,6-tetramethyl-3, 5-heptanedionate] and $Zn(hfa)_2$•TMEDA [hfa : 1,1,1,5,5,5-hexafluoro-2,4-pentanedionate; TEMDA : N,N,N´, N´-tetramethylethylenediamine][144]. MgCdO thin films have been grown by metal organic chemical vapor deposition (MOCVD)[145]. Feng et al. reported the synthesis of high-crystalline indium oxide (In_2O_3) nanowires by CVD method on Si (111) substrates using Carbon and In_2O_3 powders as the raw materials[146].

Laser pyrolysis

Laser pyrolysis is the process whereby laser induced pyrolysis of gaseous phase precursors occur in the process chamber. Generally gas phase precursors are employed. Although liquid reactants, in essential case, can be used either through in situ vaporization or in the form of microscale droplets formed via ultrasonication. A carrier gas like argon, transport the precursors to the process chamber where high-power laser beam (in the range of 2400 W) produces localized high temperature zones that cause the nucleation and growth of NPs[147]. The produced NPs are collected by a catcher fitted with a filter. Continuous mode CO_2 laser is mostly used in this process and therefore the process is also referred as CO_2 laser pyrolysis. ZnO nanostructures including nanorods and nanowires were synthesized using CO_2 laser heating of water-alcohol saturated solution of zinc-acetylacetonate [$Zn(AcAc)_2$] in open air[148]. Dumitrache et al. reported the synthesis of highly magnetic γ-Fe_2O_3-based NPs by laser pyrolysis from $Fe(CO)_5$ with varying O_2 and C_2H_4 flow ratios with different laser power values[149]. Oxygen abundant anatase and rutile TiO_2 NPs with high phase purity were synthesized from $TiCl_4$ and C_2H_4 gas mixtures by CO_2 laser radiation in presence of oxygen[150]. TiO_2/SnO_2 nanocomosites have also been synthesized from volatile $TiCl_4$ and $SnCl_4$ in presence of ethylene and air for oxidation[151].

Spray pyrolysis

Spray pyrolysis is another very simple CVD technique used to prepare thin and thick films, core-shell nanoclusters. Spray pyrolysis equipment involves an atomizer, precursor solution in liquid phase and substrate heater with temperature control. The liquid phase precursors are atomized via an atomizer and sprayed over a heated substrate by air flow, resulting in deposition of films over the substrate surface. Various types of atomizer such as ultrasonic atomizer (ultrasonic wave causes atomization), air blast (liquid is spread in an air stream) and electrostatic atomizer (electric field brings about the atomization) are used in spray pyrolysis. It is a relatively cheap process and the process control depends on the factors like deposition temperature, properties of the precursor solution regarding surface tension and pH of the solvent, type of atomizer etc. Nakate et al. recently reported the synthesis of nano-crystalline CdO thin film by spray

pyrolysis deposition[152]. Park et al. has also described the synthesis of SnSe–SnO_2 composite powders and SnSe nanospheres via one-pot spray pyrolysis by regulating the concentration of the Se precursor in the spray solution[153]. Son et al. reported the synthesis of multishelled Fe_2O_3 yolk–shell particles by a one-pot continuous spray pyrolysis process[154]. Báez-Rodríguez et al. very recently synthesized hexagonal ZnO nanocolumns by chemical bath deposition on previously deposited ZnO nanoseeds on Corning glass substrates at deposition temperatures from 300 to 550 °C in steps of 50 °C, by ultrasonic spray pyrolysis technique[155]. Core–shell structured NiO@TiO_2 nanopowders had also been prepared by flame spray pyrolysis[156].

Green synthesis

The biological, biogenic or green synthesis is the synthetic route for the formation of MONPs that utilizes microorganisms like bacteria, fungi, algae or different parts of the plants for the synthesis. The green synthesis is especially important over the conventional physical and chemical methods. Whereas physical methods require high temperature, high pressure and costly instrumentation, the chemical methods deal with toxic chemicals having a hazardous impact on the environment. The green synthetic route is totally free from these limitations. The processes are eco-friendly as well as sustainable and cost-effective[157].

The bacteria either use the metal precursor directly as its metabolite to produce the MONPs or induce the formation of MONPs from the precursors. The various enzymes and co-factors present in the fungal cells do the same task. Plant parts contain variety of phytochemicals, ranging from carbohydrates, terpenoids, flavonoids, amino acids etc. They play the role to transform the metal precursors to MONPs. The chemicals within the microbial cells and the phytochemicals serve the role of stabilizing agent, modifier as well as capping agent for the biogenic MONPs. The green synthesis route also involves a very simple work-up protocol for ultimate generation of the MONPs. However, in one particular aspect, this procedure has a crucial limitation, that is regarding the polydispersity of the produced MONPs. It is not always easy to control the conditions in case of biogenic synthesis to narrow down the size distribution. The intricate mechanism of biogenic synthesis varies from system to system, which renders the feasibility of establishing a generalized protocol. An important feature is self-attained within the biogenically synthesized MONPs that is regarding their biocompatibility. In this aspect the biogenic MONPs emerge out as potent candidate for medical application. The available reports of biogenic synthesis of MONPs are really enormous in number, only a few recent works are being highlighted here. Suriyara et al. reported the facile one pot green synthesis of ZrO_2 NPs at room temperature with average size between 37 nm – 51 nm using *Acinetobacter sp.*KCSI1 for the first time[158]. Kumaresan also reported a facile and green combustion synthesis of zirconia (ZrO_2) NPs using marine brownalga (seaweed) *Sargassum wightii*[159]. Marquis et al. synthesized CaO NPs using *Cissus quadrangularis* extract[160]. Agarwal et al. reported the eco-friendly synthesis of ZnO NPs using *Cinnamomum tamala* leaf extract[161]. Naz et al. reported the synthesis of CeO_2 NPs using aqueous stem extract of *R. punjabensis*[162]. Dubey et al. reported the novel green synthesis of cobalt oxide (Co_3O_4) NPs with average size around 10 nm using latex of *Calotropis procera* via simple precipitation method at room temperature[163]. Sukumar et al. very recently synthesized rice-shaped CuO NPs using *Caesalpinia bonducella* seed extract[164]. Surendra et al. synthesized rod shaped gadolinium oxide NPs (Gd_2O_3NPs) with average size of 26 ± 2 nm using methanolic extract of *Moringa oleifera* (*M oleifera*) peel[165]. Arsalani et al. synthesized Fe_3O_4 NPs by a simple green coprecipitation method at a mild temperature, using natural rubber latex extracted from *Hevea brasiliensis* as the capping agent[166]. Iron oxide NPs (Fe_2O_3–NPs) have also been synthesized using *Skimmia laureola* leaf extract in a benign way with size of the NPs in the range 56 nm to 350 nm[167]. Verma et al. reported the green synthesis of MgO NPs of size 55 ± 10 nm using the extract from a medicinal plant *Calotropis gigantean*[168]. Kganyago et al. reported the green synthesis of NiO NPs using *Monsonia burkeana*[169]. Fulekar et al. synthesized TiO_2 NPs using rhizosphere root zone microorganisms *Micrococcus lylae* (MF1), *Micrococcus aloeverae* (MF2), *Cellulosimicrobium sp*. (MF3), their consortium and the root extracts of mycorrhizal sorghum roots[170].

Conclusions

The synthetic procedures regarding production of MONPs according to morphology and properties comprise a very challenging domain. Based on the generalized principles of synthesis, new routes are being innovated where two or more synthetic

protocols are being utilized in a single synthesis according to the need. The main aim remains always to use an eco-friendly set up with narrow polydispersity and increased biocompatibility. The instrumentation for characterization of NPs is improving generously and finer details of NPs are being explored – this also triggers towards synchronization and innovation of newer synthetic routes for the production of MONPs.

References

1 Technical Fact Sheet – Nanomaterials November 2017, https://www.epa.gov/sites/production/files/2014-03/documents/ffrrofactsheet_emergingcontaminant_nanomaterials_jan2014_final.pdf.
2 Lövestam G, Rauscher H, Roebben G, Klüttgen B S, Gibson N, Putaud J -P & Stam H, *JRC Reference Reports, Considerations on a Definition of Nanomaterial for Regulatory Purposes*, (2010) 13.
3 Commission Recommendation of 18 October 2011 on the definition of nanomaterial 2011/696/EU. *Off J Eur Union*, L 275 (2011) 38.
4 Pettibone J M, Baltrusaitis J & Grassian V H, *Synthesis, Properties and Applications of Oxide Nanomaterials*, (John Wiley & Sons, Inc., Hoboken, New Jersey) 2007, pp. 1.
5 Ayyub P, Palkar V R, Chattopadhyay S & Multani M, *Phys Rev B*, 51 (1995) 6135.
6 McHale J M, Auroux A, Perrota A J & Navrotsky A, *Science*, 277 (1997) 788.
7 Samsonov V M, Sdobnyakov N Y & Bazulev A N, *Surf Sci*, 532 (2003) 526.
8 Cammarata R C & Sieradki K, *Phys Rev Lett*, 62 (1989) 2005.
9 Fernández-García M, Wang X, Belver C, Hanson A, Iglesias-Juez J C & Rodriguez J A, *Chem Mater*, 17 (2005) 4181.
10 Moriarty P, *Rep Prog Phys*, 64 (2001) 297.
11 Yoffre A D, *Adv Phys*, 42 (1993) 173.
12 Fernández-García M, Conesa J C & Illas F, *Surf Sci*, 349 (1996) 207.
13 Albaret T, Finocchi F & Noguera C, *Faraday Discuss*, 114 (2000) 285.
14 Rodriguez J A, *Theor Chem Acc*, 107 (2002) 117.
15 Rodriguez J A, Chaturvedi S, Kuhn M and Hrbek J, *J Phys Chem B*, 102 (1998) 5511.
16 Hoffmann R, *Solids and Surfaces: A Chemist's View of Bonding in Extended Structures*, (VCH, NewYork) 1988.
17 Luth H, *Surface and Interface of Solid Materials*, (Springer, Berlin) 1997.
18 Richards R, Li W, Decker S, Davidson C, Koper O, Zaikovski V, Volodin A & Rieker T, *J Am Chem Soc*, 122 (2000) 4921.
19 Chavali M S & Nikolova M P, *SN Applied Sciences*, 1 (2019) 1.
20 Pettibone J M, Baltrusaitis J & Grassian V H, *Synthesis, Properties and applications of oxide nanomaterials*, (John Wiley & Sons, Inc., Hoboken, New Jersey) 2007, pp. 335.
21 Noguera C, *Physics and Chemistry at Oxide Surfaces*, (Cambridge University Press, Cambridge, UK) 1996.
22 Richards R M, *Dekker Encyclopedia of Nanoscience and Nanotechnology*, (CRC Press, Boca Raton, USA) 2014, pp. 1905.
23 Rao C N R, Matte H S S R, Voggu R & Govindaraj A, *Dalton Trans*, 41 (2012) 5089.
24 Kapoor P N, Bhagi A K, Mulukutla R S & Klabunde K, *Dekker Encyclopedia of Nanoscience and Nanotechnology*, (CRC Press, Boca Raton, USA) 2014, pp. 2007.
25 Gaskov A & Rumyantseva M, *Sensors for Environment, Health and Security. NATO Science for Peace and Security Series C: Environmental Security*, (Springer, Dordrecht) 2009, pp. 3.
26 Parnianchi F, Nazari M, Maleki J & Mohebi M, *Int Nano Lett*, 8 (2018) 229.
27 Jana A, Scheer E & Polarz S, *Beilstein J Nanotechnol*, 8 (2017) 688.
28 Atisme T B, Yu C –Y, Tseng E N, Chen Y –C, Hsu P –K & Chen S –Y, *Nanomaterials(Basel)*, 9 (2019) 1534.
29 Rahman M T, Hoque M A, Rahman G T, Gafur M A, Khan R A & Hossain M K, *Results Phys*, 13 (2019) 102264.
30 Sosa-Acosta J R, Iriarte-Mesa C, Ortega G A & Diaz-Garcia A M, *Top Curr Chem*, 378 (2020) Article Number 13.
31 Magro M, Martinello T, Bonaiuto E, Gomiero C, Baratella D, Zoppellaro G, Cozza G, Patruno M, Zboril R & Vianello F, *BBA-GEN SUBJECTS*, 1861 (2017) 2802.
32 Skorjanc T, Benyettou F, Olsen J & Trabolsi A, *Chem Eur J*, 23 (2017) 8333.
33 Falcaro P, Ricco R, Yazdi A, Imaz I, Furukawa S, Maspoch D, Ameloot R, Evans J D & Doonan C J, *Coord Chem Rev*, 307 (2016) 237.
34 Kumar D K, Kriz J, Bennett N, Chen B, Upadhayaya H, Reddy K R & Sadhu V, *Mater Sci Ener Technol*, 3 (2020) 472.
35 Abu-Dief A M, *J Nanotechnol Nanomater*, 1 (2020) 5.
36 Gerken L R H, Keevend K, Zhang Y, Starsich F H L, Eberhardt C, Panzarasa G, Matter M T, Wichser A, Boss A, Neels A & Herrmann I K, *ACS Appl Mater Interfaces*, 11 (2019) 437.
37 Zhang H, Ji Z, Xia T, Meng H, Low-Kam C, Liu R, Pokhrel S, Lin S, Wang X, Liao Y, Wang M, Li L, Rallo R, Damoiseaux R, Telesca D, Mädler L, Cohen Y, Zink J I & Nel A E, *ACS Nano*, 6 (2012) 4349.
38 Gao Y, Zhou Y & Chandrawati R, *ACS Appl Nano Mater*, 3 (2020) 1.
39 Pal S & Jana N R, *ACS Appl Nano Mater*, 3 (2020) 1683.
40 Archana V, Xia Y, Fang R & Kumar G G, *ACS Sustain Chem Eng*, 7 (2019) 6707.
41 Adithya G T, Rangabhashiyam S & Sivasankari C, *Microchem J*, 148 (2019) 364.
42 Gnanasekaran L, Hemamalini R, Saravanan R, Ravichandran K, Garcia F, Agarwal S & Gupta V K, *J Photoch Photobio B*, 173 (2017) 43.
43 Gonçalves R V, Wender H, Migowski P, Feil A F, Eberhardt D, Boita J, Khan S, Machado G, Dupont J & Teixeira S R, *J Phys Chem C*, 121 (2017) 5855.
44 Benjamin J T, *Sci Amer*, 234 (1976) 40.
45 Lee J S, Lee C S, Oh S T & Kim J G, *Scripta Mater*, 44 (2001) 2023.
46 Indris S, Amade R, Heitjans P, Finger M, Haeger A, Hesse D, Grünert W, Börger A & Becker K D, *J Phys Chem B*, 109 (2005) 23274.
47 Avvakumov E G & Karakchiev L G, *Chem Sustainable Dev*, 12 (2004) 287.
48 Seyedi M, Haratian S & Khaki J V, *Procedia Mater Sci*, 11 (2015) 309.
49 Li Y X, Chen W F, Zhou X Z, Gu Z Y & Chen C M, *Mater Lett*, 59 (2005) 48.
50 Lu J, Ng K M & Yang S, *Ind Eng Chem Res*, 47 (2008) 1095.
51 Shi Y, Ding J & Yin H, *J Alloys Compd*, 308 (2000) 290.

52 Priyadarshana G, Kottegoda N, Senaratne A, deAlwis A & Karunaratne V, *J Nanomater*, (2015) 1.
53 He H, Cao J, Fei X & Duan N, *Environ Int*, 130 (2019) 104930.
54 Zhou Y, Dong C-K, Han L-L, Yang J & Du X-W, *ACS Catal*, 6 (2016) 6699.
55 Wang H Q, Li G H, Jia L C, Wang G Z & Li L, *Appl Phys Lett*, 93 (2008) 153110.
56 An K, Kwon S G, Park M & Na H B, *Nano Lett*, 8 (2008) 4252.
57 Li P, Yan X, He Z, Ji J, Hu J, Li G, Lian K & Zhang W, *CrystEngComm*, 18 (2016) 1752.
58 Hotovy I, Kostic I, Predanocy M, Nemec P & Rehacek V, *J Electr Eng*, 67 (2016) 454.
59 Eugene L A, Mariagoretti O U & Samuel B A, *Chem Res J*, 2 (2017) 97.
60 Nikam A V, Prasad B L V & Kulkarni A A, *CrystEngComm*, 20 (2018) 5091.
61 Bang J H & Suslick K S, *Adv Mater*, 22 (2010) 1039.
62 Hosseini S G & Khodadadipoor Z, *Indian J Chem*, 57A (2018) 449.
63 Duraisamy N, Numan A, Fatin S O, Ramesh K & Ramesh S, *J Colloid Interface Sci*, 471 (2016) 136.
64 Arami H, Mazloumi M, Khalifehzadeh R & Sadrnezhaad S K, *Mater Lett*, 61 (2007) 4559.
65 Yin L, Wang Y, Pang G, Koltypin Y and Gedanken A, *J Colloid Interface Sci*, 246 (2002) 78.
66 Massart R & Cabuil V, *J Chim Phys Phys Chim Biol*, 84 (1987) 967.
67 Adam R E, Pozina G, Willander M, Nur O, *Photonic Nanostruct*, 32 (2018) 11.
68 Jamil S, Khan S R, Sultana B, Hashmi M & Haroon M, *J Clust Sci*, 29 (2018) 1099.
69 Nejati K, *Cryst Res Technol*, 47 (2012) 567.
70 Smith S J, Huang B, Liu S, Liu Q, Olsen R E, Boerio-Goates J & Woodfield B F, *Nanoscale*, 7 (2015) 144.
71 Sharma M, Pathak M & Kapoor P N, *Asian J Chem*, 30 (2018) 1405.
72 Kang O L, Ahmad A, Rana U A & Hassan N H, *J Nanotechnol*, (2016), Article ID 5375939.
73 Tyagi B, Sidhpuria K, Shaik B & Jasra R V, *Ind Eng Chem Res*, 45 (2006) 8643.
74 Athar T, Hakeem A & Ahmed W, *Adv Sci Lett*, 5 (2012) 1.
75 Zhang L Z, Djerdj I, Cao M & Antonietti M, *Adv Mater*, 19 (2007) 2083.
76 Malik M A, Wani M Y & Hashim M A, *Arab J Chem*, 5 (2012) 397.
77 Ganguli A K, Ganguly A & Vaidya S, *Chem Soc Rev*, 39 (2010) 474.
78 Sarkar D, Tikku S, Thapar V & Srinivasa R S, *Colloid Surface A*, 381 (2011) 123.
79 Bumajdad A, Zaki M I, Eastoe J & Pasupulety L, *Langmuir*, 20 (2004) 11223.
80 Dodoo-Arhin D, Leoni M & Scardi P, *Mol Cryst Liq Cryst*, 555 (2012) 17.
81 Li J, Wu Q & Wu J, *Handbook of Nanoparticles* (Springer, Cham) 2015, pp. 1.
82 Rai P, Kwak W & Yu Y, *ACS Appl Mater Interfaces*, 5 (2013) 3026.
83 Mishra D, Arora R, Lahiri S, Amritphale S S & Chandra N, *Prot Met Phys Chem Surf*, 50 (2014) 628.
84 Aguilar T, Carrillo-Berdugo I, Gómez-Villarejo R, Gallardo J J, Martínez-Merino P, Piñero J C, Alcántara R, Fernández-Lorenzo C & Navas J, *Nanomaterials*, *8 (*2018) 816.
85 Pang J, Liu Y, Li J & Yang X, *Rare Metals*, 38 (2019) 73.
86 Kim J H, Noh B H, Lee G & Hong S, *Korean J Chem Eng*, 22 (2005) 370.
87 Hsu Y F, Xi Y Y, Tam K H, Djurišić A B, Luo J, Ling C C, Cheung C K, Ching Ng A M, Chan W K, Deng X, Beling C D, Fung S, Cheah K W, Fong P W K & Surya C C, *Adv Func Mater*, 18 (2008) 1020.
88 Duong T H Y, Nguyen T N, Oanh H T, Thi T A D, Giang L N T, Phuong H T, Anh N T, Nguyen B M, Quang V T, Le G T & Nguyen T V, *J Chem*, (2019), Article ID 4376429.
89 Yang Y, Wang X, Yi G, Li H, Shi C, Sun G & Zhang Z, *Nanomaterials*, 9 (2019) 1599.
90 Li F, Ran J, Jaroniec M & Qiao S Z, *Nanoscale*, 7 (2015) 17590.
91 Wang X, Qin M, Fang F, Jia B, Wu H, Qu X & Volinsky A A, *Ceram Int*, 44 (2018) 4237.
92 (a) Vasei H V, Masoudpanah S M, Adeli M & Aboutalebi M R, *Ceram Int*, 44 (2018) 7741; (b) Vasei H V, Masoudpanah S M, Adeli M & Aboutalebi M R, *JSST*, 89 (2019) 586.
93 Balamurugan M, Silambarasan M, Saravanan S & Soga T, *AIP Conf Proc*, 1665 (2015) 050116.
94 Balamurugan S, Ashna L & Parthiban P, *J Nanotechnol*, (2014), Article ID 841803.
95 Singh A K & Nakate U T, *Adv Nanoparticles*, 2 (2013) 66.
96 Zhong G, Xu S, Chen C, Kline D J, Giroux M, Pei Y, Jiao M, Liu D, Mi R, Xie H, Yang B, Wang C, Zachariah M R & Hu L, *Adv Funct Mater*, 29 (2019) 1904282.
97 Li X, Ding N, Lu Y & Yin X J, *ChemistrySelect*, 3 (2018) 8553.
98 Barreto G, Morales G, Cañizo A & Eyler N, *Procedia Mater Sci*, 8 (2015) 535.
99 Vijayakumar S, Ponnalagi A K, Nagamuthu S & Muralidharan G, *Electrochim Acta*, 106 (2013) 500.
100 Park H, Ayala P, Deshusses M A, Mulchandani A, Choi H & Myung N V, *Chem Eng J*, 139 (2008) 208.
101 Yang Q, Long M, Tan L, Zhang Y, Ouyang J, Liu P & Tang A, *ACS Appl Mater Interfaces*, 7 (2015) 12719.
102 Yu W C, Sabastian N, Chang W C, Tsia C Y & Lin C M, *J Nanosci Nanotechnol*, 18 (2018) 56.
103 Costovici S, Petica A, Dumitru C S, Cojocaru A & Anicai L, *Chem Eng Trans*, 41 (2014) 343.
104 Fedorov F S, Podgainov D, Varezhnikov A & Lashkov A V, *Sensors*, 17 (2017) 1908.
105 Ramsden J J, *Nanotechnology An Introduction Micro & Nano Technologies*, (William Andrew Applied Science Publishers) 2011, pp. 101.
106 Halbedel B, Prikhna T, Quiroz P, Schawohl J, Kups T & Monastyrov M, *Curr Appl Phys*, 18 (2018) 1410.
107 Huczko A, *Appl Phys A*, 70 (2000) 365.
108 Qi D, Chu H, Wang K, Li X & Huang J, *ChemistrySelect*, 3 (2018) 12469.
109 Li Y, Song K, Cao Y, Peng C & Yang G, *ACS Appl Mater Interfaces*, 10 (2018) 26039.
110 Sharma S, Kulkarni P & Kumar R, *Luminescence*, 31 (2016) 978.
111 Kumar K, Chen B, Xuan J, Maroto-Valer M M, Leung D Y C & Wang H, *ChemistrySelect*, 2 (2017) 702.
112 Manukyan K V, Chen Y, Rouvimov S, Li P, Li X, Dong S, Liu X, Furdyna J K, Orlov A, Bernstein G H, Porod W, Roslyakov S & Mukasyan A S, *J Phys Chem C*, 118 (2014) 16264.
113 Fouad O, Ismail A, Zaki Z & Mohamed R M, *Appl Catal B*, 62 (2006) 144.
114 Zhang Y, Wang L, Liu X, Yan Y, Chen C & Zhu J, *J Phys Chem B*, 109 (2005) 13091.

115 Al-Kuhaili M F, Saleem M & Durrani S M A, *J Alloys Compd*, 521 (2012) 178.
116 Al-Kuhaili M F, *Vacuum*, 82 (2008) 623.
117 Oboudi S F, Habubi N F, Ni'ma A H & Chiad S S, *NSNTAIJ*, 8 (2014) 320.
118 Yang T, Shiu C & Wong M, *Surface Sci*, 548 (2004) 75.
119 Tesfamichael T, Arita M, Bostrom T & Bell J, *Thin Solid Films*, 518 (2010) 4791.
120 Basnet P, Larsen G K, Jadeja R P, Hung Y & Zhao Y, *ACS Appl Mater Interfaces*, 5 (2013) 2085.
121 Swann S, *Phys Technol*, 19 (1988) 67.
122 Chuang K T, Abdullah H, Leu S J, Cheng K B, Kuo D H, Chen H C, Chien J H & Hu W T, *J Photoch Photobio A*, 337 (2017) 151.
123 Shivya P, Prasad A K & Sridharan M, *J Solid State Chem*, 214 (2014) 24.
124 Rydosz A, Brudnik A & Staszek K, *Materials*, 12 (2019) 877.
125 Diaz B, Światowska J, Maurice V & Pisarek M, *Surf Coat Tech*, 206 (2012) 3903.
126 Zhirkov I S, Paternoster C & Delplancke-Ogletree M P, *Journal of Physics: Conference Series*, 275 (2011) 012019.
127 Aramwit C, Intarasiri S, Bootkul D, Tippawan U, Supsermpol B, Seanphinit N, Ruangkul W & Yu L D, *Journal of Physics: Conference Series*, 423 (2013) 012005.
128 Marquez A, Blanco G, Fernandez de Rapp M E & Lamas D G, *Surf Coat Tech*, 187 (2004) 154.
129 Camarda P, Vaccaro L, Sciortino A, Messina F, Buscarino G, Agnello S, Gelardi F M, Popescu R, Schneider R, Gerthsen D & Cannas M, *Appl Surf Sci*, 506 (2020) 144954.
130 Gondal M A, Drmosh Q A & Saleh T A, *Appl Surf Sci*, 256 (2010) 7067.
131 Zuñiga-Ibarra V A, Shaji S, Krishnan B, Johny J, Kanakkillam S S, Avellaneda D A, AguilarMartinez J A, Das Roy T K & Ramos-Delgado N A, *Appl Surf Sci*, 483 (2019) 156.
132 Mostafa A M, Yousef S A, Eisa W H, Ewaida M A & Al-Ashkar E A, *Optik*, 144 (2017) 679.
133 Ramasamy S, Smith D J, Thangadurai P, Ravichandran K, Prakash T, Padmaprasad K & Sabarinathan V, *Pramana-J Phys*, 65 (2005) 881.
134 Kusior A, Kollbek K, Kowalski K, Borysiewicz M, Wojciechowski T, Adamczyk A, Trenczek-Zajac A, Radecka M & Zakrzewska K, *Appl Surf Sci*, 380 (2016) 193.
135 Ayesh A I, *Thin Solid Films*, 636 (2017) 207.
136 Uhm Y R, Han B S, Lee M K, Hong S J & Rhee C K, *Mat Sci Eng A*, 449-451 (2007) 813.
137 Vaghayenegar M, Kermanpur A & Abbasi M H, *Ceram Int*, 38 (2012) 5871
138 Uhm Y R, Kim W W & Rhee C K, *Physica Status Solidi A*, 201 (2004) 1934.
139 Uhm Y R, Han B S, Lee H M & Rhee C K, *Solid state Phenomena*, 135 (2008) 123.
140 Hussain A, Gruehn R & Rüscher C H, *J Alloy Compd*, 246 (1997) 51.
141 Wang X, Ding Y, Summers C J & Wang Z L, *J Phys Chem B*, 108 (2004) 8773.
142 Patelli N, Migliori A, Morandi V & Pasquini L, *Nanomaterials(Basel)*, 9 (2019) 219.
143 Bekermann D, Barreca D, Gasparotto A & Maccato C, *CrystEngComm*, 14 (2012) 6347.
144 Barreca D, Comini E, Ferrucci A P, Gasparotto A, Maccato C, Maragno C, Sberveglieri G & Tondello E, *Chem Mater*, 19 (2007) 5642.
145 Guia L M, Sallet V, Hassani S, Martínez-Tomás M C & Muñoz-Sanjosé V, *Cryst Growth Des*, 17 (2017) 6303.
146 Feng C, Liu X, Wen S & An Y, *Vacuum*, 161 (2019) 328.
147 Arulmani S, Anandan S & Ashokkumar M, *Nanomaterials for Green Energy*, (Imprint–Elseveir) 2018, pp. 1
148 Fauteux C, Longtin R, Pegna J & Therriault D, *Inorg Chem*, 46 (2007) 11036.
149 Dumitrache F, Morjan I, Fleaca C, Badoi A, Manda G, Pop S, Marta D S, Huminic G, Huminic A, Vekas L, Daia C, Marinica O, Luculescu C & Niculescu A, *Appl Surf Sci*, 336 (2015) 297.
150 Ilie A G, Scarisoreanu M, Dutu E, Dumitrache F, Banici A, Fleaca C T, Vasile E & Mihailescu I, *Appl Surf Sci*, 427A (2018) 798.
151 Scarisoreanu M, Fleaca C, Morjan I, Niculescu A, Luculescu C, Dutu E, Ilie A, Morjan I, Florescu L G, Vasile E & Fort C I, *Appl Surf Sci*, 418B (2017) 491.
152 Nakate U T, Patil P, Ghule B, Nakate Y T, Ekar S, Ambare R C & Mane R S, *Surf Interfaces*, 17 (2019) 100339.
153 Park G D, Kim J H & Kang Y C, *Nanoscale*, 10 (2018) 13531.
154 Son M Y, Hong Y J, Lee J & Kang Y C, *Nanoscale*, 5 (2013) 11592.
155 Báez-Rodríguez A, Zamora-Peredo L, Soriano-Rosales M G, Hernández-Torres J, García-González L, Calderón-Olvera R M, García-Hipólito M, Guzmán-Mendoza J & Falcony C, *J Lumin*, 218 (2020) 116830.
156 Choi S H, Lee J & Kang Y C, *Nanoscale*, 5 (2013) 12645.
157 Zikalala N, Matshetshe K, Parani S & Oluwafemi O S, *Nano-Structures & Nano-Objects*, 16 (2018) 288.
158 Suriyara S P, Ramadoss G, Chandraraj K & Selvakumar R, *Mater Sci Eng C*, 105 (2019) 110021.
159 Kumaresan M, Anand K V, Govindaraju K, Tamilselvan S & Kumar V G, *Microbial Pathogenesis*, 124 (2018) 311.
160 Marquis G, Ramasamy B, Banwarilal S and Munusamy A P, *J Photoch Photobio B*, 155 (2016) 28.
161 Agarwal H, Nakara A, Menon S & Shanmugam V K, *J Drug Deliv Sci Technol*, 53 (2019) 101212.
162 Naz S, Kazmi S T B & Zia M, *J Biochem Mol Toxicol*, 33 (2019) e22291.
163 Dubey S, Kumar J, Kumar A & Sharma Y C, *Adv Powder Technol*, 29 (2018) 2583.
164 Sukumar S, Rudrasenan A & Nambiar D P, *ACS Omega*, 5 (2020) 1040.
165 Surendra T V, Roopan S M & Khan M R, *Biotechnol Progress*, 35 (2019) e2823.
166 Arsalani S, Guidelli E J, Araujo J F D F, Bruno A C & Baffa O, *ACS Sustainable Chem Eng*, 6 (2018) 13756.
167 Alam T, AliKhan R A, Ali A, Sher H, Ullah Z & Ali M, *Mater Sci Eng C*, 98 (2019) 101.
168 Verma S K, Nisha K, Panda P K, Patel P, Kumari P, Mallick M A, Sarkar B & Das B, *Sci Total Environ*, 713 (2020) 136521.
169 Kganyago P, Mahlaule-Glory L M, Mathipa M M, Ntsendwana B, Mketo N, Mbita Z & Hintsho-Mbita N C, *J Photoch photobio B*, 182 (2018) 18.
170 Fulekar J, Dutta D P, Pathak B & Fulekar M H, *J Chem Technol Biotechnol*, 93 (2018) 736.